RESEARCH ARTICLE
doi: 10.2306/scienceasia1513-1874.2024.047

ScienceAsia 50 (2): 2024: ID 2024047: **1–7**

Saccharibacillus mori sp. nov., a novel indole-3-acetic acid-producing and phosphate-solubilizing bacterium isolated from a medicinal plant rhizosphere soil

Xue-Fei Han[a,b], **Yang Deng**[a,b], **Li-Yan Yu**[a], **Hua-Hong Chen**[c,*], **Yu-Qin Zhang**[a,b,*]

[a] Institute of Medicinal Biotechnology, Chinese Academy of Medical Sciences & Peking Union Medical College, Beijing 100050 China
[b] State Key Laboratory of Dao-di Herb, Beijng 100700 China
[c] Department of Chemistry and Biology Science, Chuxiong Normal University, Chuxiong, Yunnan 675000 China

[*]Corresponding authors, e-mail: huahongc@gmail.com, zhyuqin@126.com

Received 1 Aug 2023, Accepted 13 Jan 2024
Available online 3 May 2024

ABSTRACT: A Gram-positive, rod-like, and aerobic bacterium labeled JD154^T was recovered from the rhizosphere soil of a mulberry tree, a medicinal plant, in Yunnan Province, China. It proved a closely knit relationship to the genus *Saccharibacillus* via the 16S rRNA gene sequence comparison, showing the highest similarity of 96.4% to *Saccharibacillus kuerlensis* DSM 22868^T and *Saccharibacillus sacchari* DSM 19268^T. The considerate low average nucleotide identity (77.1–80.0%) and digital DNA-DNA hybridization values (17.7–25.6%) with other *Saccharibacillus* strain genomes indicated strain JD154^T as a new genetic species. It grew effectively between 10–37 °C and a pH range of 5.0–9.0, optimally thriving at 20–30 °C and a pH of 7.0–8.0. Major cellular fatty acids found in the strain were *anteiso*-$C_{15:0}$, $C_{16:0}$, *iso*-$C_{14:0}$, and *iso*-$C_{15:0}$. The primary respiratory quinone documented was menaquinone-7, and the polar lipids were diphosphatidylglycerol and phosphatidylglycerol. Evaluation of its genome revealed gene clusters potentially involved in processes such as phosphate solubilization and indole acetic acid biosynthesis. Evidence of these plant growth-promoting characteristics was confirmed by indole-3-acetic acid (IAA) production (11.04 ± 0.04 μg/ml) and phosphate-solubilizing (P-solubilizing) activity. Taking into account the unique genetic and phenotypic characteristics, strain JD154^T is suggested to represent a novel species within the genus *Saccharibacillus*, proposed to be titled *Saccharibacillus mori* sp. nov.

KEYWORDS: *Saccharibacillus mori*, polyphasic taxonomy, phosphate solubilization, indole-3-acetic acid

INTRODUCTION

Rivas et al initially proposed the genus *Saccharibacillus* [1] with its description, later revised by Sun et al [2] upon observing the enzymic characteristics of *S. deserti* WLJ055^T. This genus is characterized by Gram-stain-variable, facultatively anaerobic, and rod-shaped attributes with menaquinone-7 as the key respiratory quinone and *anteiso*-$C_{15:0}$ as the predominant fatty acid. Currently, *Saccharibacillus*, a genus hosting 5 validly described species (https://lpsn.dsmz.de/genus/Saccharibacillus), includes type strains from varied ecosystems, ranging from the apoplastic fluid of *Saccharum officinarum* [1] to desert soil [3], lead-cadmium tailing soil [4], and the inner tissues of field-grown cotton [5]. Recent studies by Bziuk et al [6] found *Saccharibacillus* spp. to be the principal bacteria in the barley seed microbiome via 16S rRNA gene amplicon sequencing.

This research detailed our findings from the isolation of strain JD154^T from the soil of rhizosphere of a medicinal plant (mulberry tree), identification of it as a new species within the genus *Saccharibacillus* based on physiological, chemotaxonomic, and phylogenetic features. Together with this discovery, we delved into the plant growth-promoting potential of strain JD154^T by exploring genes linked to IAA biosynthesis and phosphate solubilization. We confirmed these characteristics through functional tests by IAA production and phosphate solubilization.

MATERIALS AND METHODS

Acquisition and identification of the microorganisms

Strain JD154^T was obtained from rhizosphere soil of a mulberry tree in Yuxi city, Yunnan Province, China, a region located at the geographical coordinates of 101°43′5″ E and 24°20′3″ N. The strain was isolated using the methodology outlined by Jiang et al [7]. Selection of distinctive colonies from the isolation plates was carried out, followed by streaking onto freshly made peptone-yeast extract-glycerol (PYG) agar slants (g/l: peptone 3, yeast extract 5, glycerol 10, betaine hydrochloride 1.25, sodium pyruvate 1.25, agar 15, pH 7.2) [7]. The purified strains were then preserved on PYG agar at 4 °C and in glycerol suspensions (20% v/v) at −80 °C.

The genomic DNA from the strain JD154^T was extracted, and the 16S rRNA gene was amplified using a methodology described by Li et al [8]. The amplified product was sequenced by Sangon Biotech (Shanghai, China). The resulting sequence was compared to the available 16S rRNA gene sequences in Gen-

Bank using BLAST and the EzTaxon-e server, to ascertain its likely taxonomic standing. Subsequent multi-sequence alignments and phylogenetic reconstructions were done with MEGA (version 11) [9]. Construction of a phylogenetic tree involved a neighbor-joining method [10], employing K values, and complete gap deletion [11, 12]. Maximum parsimony [13] and maximum-likelihood [14] algorithms were also used for phylogenetic consideration of the strain. Bootstrap analysis based on 1,000 random replicates [15] was used to confirm tree robustness.

Parallel assays incorporated reference strains *S. kuerlensis* DSM 22868^T and *S. sacchari* DSM 19268^T, sourced from the German Collection of Microorganisms and Cell Cultures GmbH (DSMZ).

Morphological and physiological characterization

Growth medium tests

In order to thoroughly understand the growth properties of the isolate and contribute to its taxonomy, strain JD154^T was cultured under different conditions on various agar media. These included nutrient agar, tryptone soy agar (TSA; Difco, Sparks, USA), Reasoner's 2A agar (R2A; Difco), Luria-Bertani agar (LB; Difco), and International Streptomyces Projects Medium 2 (ISP 2; Difco) [16].

Temperature, pH, and NaCl tolerance tests

Tests were conducted to measure the isolate optimal temperature and pH growth range and salt tolerance, following the methods described previously [8].

Gram staining and microscopic observation

Gram staining was performed, followed by observations under the light microscope (Axio A1 Vario, Zeiss, Oberkochen, Germany). Motility of the cells was examined using the semisolid nutrient agar medium (SNA) (g/l: peptone 10, beef extract 3, NaCl 5, agar 3, pH 7.2) and the hanging drop method [17]. Morphological characteristics of the cells were examined using transmission electron microscopy (JEOL JEM-1010, Tokyo, Japan).

Carbon assimilation tests and metabolic characterization

Carbon compound assimilation ability was tested using GEN III Microplates (Biolog, USA). The oxidase activity was detected using Analytical Profile Index oxidase reagent (API; bioMérieux, Craponne, France) according to the manufacturer's instructions. Catalase activity was assessed by evaluating the production of bubbles with addition of a drop of 3% (v/v) hydrogen peroxide. Tests for hydrolysis of cellulose and starch, gelatin liquefaction, milk coagulation and peptonization, and nitrate reduction were performed as Dong et al [18]. Voges-proskauer (VP) [19] and methyl-red (MR) [20] tests were performed using glucose-peptone broth medium. Other metabolic tests were conducted using API 50CH and API ZYM test kits. Tests for specific physiological and metabolic traits were performed such as IAA production and P-solubilizing ability, which might be leveraged for plant growth promotion. The ability of the strain to produce IAA was assessed using colorimetric methods [21, 22]. For evaluation of P-solubilizing ability, strain JD154^T was cultured on TSA plates for 48 h at 28 °C, followed by spot-inoculation on National Botanical Research Institute's phosphate growth medium (NBRIP) (g/l: glucose 10, $Ca_3(PO_4)_2$ 5, $MgCl_2$ 5, $MgSO_4 \cdot 7H_2O$ 0.25, KCl 0.2, $(NH_4)_2SO_4$ 0.1, agar 15, pH 7.0). After incubation at 28 °C for 7 days, the phosphate halo diameter (HD) and colony diameter (CD) were measured, and the HD/CD value was calculated. The presence of a phosphate halo indicated P-solubilizing ability with a value of HD/CD > 1 considered as the criterion for colony selection. HD/CD > 1.5 indicated a strong P-solubilizing ability [23].

Chemotaxonomic properties

Cell biomass collection

The cell biomass was collected from tryptic soy broth (TSB) at 28 °C until the cells reached exponential growth phase (48 h).

Polar lipid extraction and identification

Polar lipids were extracted [24] and then separated using two-dimensional thin layer chromatography (TLC), a method commonly used to distinguish between different classes of lipids based on their chemical properties and mobility [24].

Visualization of lipids

Following TLC, various lipid classes were identified using different staining techniques. (i) General lipids: Visualized using a molybdatophosphoric acid solution. (ii) Aminolipids: Revealed using a ninhydrin solution. (iii) Phospholipids: Detected with molybdenum blue. (iv) Glycolipids: Identified using α-naphthol solution.

Menaquinones extraction and analysis

The menaquinones were isolated using a method by Collins et al [25] and then analyzed using high-pressure liquid chromatography (HPLC) [26].

Fatty acid profile analysis

Cellular fatty acids were extracted according to the protocol [27] and identified using gas chromatography (Agilent 6890N, Santa Clara, USA) with the help of Sherlock Microbial Identification System using the database (TSBA6) for comparison [27].

Genome sequencing and basic analysis

The whole-genome sequencing was executed using Illumina HiSeq 4000 system (Illumina, SanDiego, CA, USA) at the Beijing Genomics Institute (Beijing, China). The library construction process included randomly shearing the genomic DNA by a Bioruptor ultrasonicator (Diagenode, Denville, NJ, USA) and physico-chemical methods, leading to the creation of read libraries.

The sequenced reads were then assembled using SOAPdenovo v1.05 software. A set of contigs from the short-read sequencing data was produced, which were sequences of contiguous DNA bases obtained from a particular read. Then, the genome quality was estimated by the CheckM pipeline, which offered a robust and extensive approach to ensure the understanding of the quality of microbial genomes recovered from a single isolate. Calculation of Digital DNA-DNA hybridization (dDDH) values and average nucleotide identity (ANI) values was conducted using the Genome-to-Genome Distance Calculator (GGDC, version 3.0; http://ggdc.dsmz.de/ggdc.php) [28] and the ezbiocloud platform [29], respectively, to compare the isolate with other relevant strains. For the construction of a reliable core gene phylogeny, EasyCGTree software package (https://github.com/zdf1987/EasyCGTree4) was used under the Windows operating system (OS). The algorithm used in this software was initially introduced by Zhang et al [30]. The evolutionary distance was calculated using IQ-Tree 1.6.1 software [31]. After the construction of robust core gene phylogeny, gene prediction was carried out on the genome assembly using glimmer3 (http://www.cbcb.umd.edu/software/glimmer), which employed Hidden Markov models. The recognition of tRNA, rRNA, and sRNAs was determined by tRNAscan-SE [32], RNAmmer, and the Rfam database, respectively. Tandem repeat annotation was performed using the Tandem Repeat Finder (http://tandem.bu.edu/trf/trf.html). Lastly, functional and pathway analyses allowed us to understand the functionalities of specific genes and their active involvement in different biological pathways. The genome sequences of the reference strains facilitated providing a broader context to compare and understand genomic data. To gain insights into the functionality and pathways, functional and pathway analyses were performed using the BlastKOALA web tool of the KEGG database [33]. Predictions of gene clusters involved in natural product formation were accomplished using antiSMASH 7.0 [34]. The reference genome sequences were downloaded from the NCBI genome database (https://www.ncbi.nlm.nih.gov/genome).

RESULTS AND DISCUSSION

Morphological and physiological characteristics

Strain JD154^T grew well on TSA, LB, R2A, and ISP 2 at 28 °C. Growth occurred on TSA at 10–37 °C (optimum 20–30 °C), 0–7% NaCl (optimum 0–1% NaCl), and pH 5.0–9.0 (optimum pH 7.0–8.0). After 48 h of cultivation at 28 °C, colonies of strain JD154^T on TSA appeared circular (0.9–1.2 mm in diameter), light-pink, convex, and opaque. The cells were motile, rod-shaped with lophotrichous flagella, and Gram-stain-positive. Cells were found to be approximately 0.8–1.1 μm in width and 2.0–3.9 μm in length (Fig. S1). This strain was positive for catalase activity and negative for oxidase activity, cellulose hydrolysis, starch hydrolysis, H_2S production, nitrate reduction, gelatin liquefaction, milk coagulation and peptonization, and VP and MR tests. Notably, the strain showcased the ability to produce IAA and solubilize phosphorus. According to the linear regression equation ($y = 0.0255x + 0.0411$, $R^2 = 0.9992$) (Fig. S2), the IAA content generated by strain JD154^T was calculated to be 11.04 ± 0.04 μg/ml, in the tryptone-yeast extract-$CaCl_2$ (TYC) broth medium (g/l: tryptone 5, yeast extracts 3, $CaCl_2 \cdot 2H_2O$ 0.872, L-tryptophan 0.612). The P-solubilizing activity test revealed HD/CD values of 1.4 ± 0.1 for strain JD154^T, indicating its moderate ability to solubilize phosphorus.

Chemotaxonomy

The major polar lipids of the strain were identified as diphosphatidylglycerol (DPG) and phosphatidylglycerol (PG) (Fig. S3). The primary fatty acid composition included *anteiso*-$C_{15:0}$ (52.8%), $C_{16:0}$ (12.0%), *iso*-$C_{14:0}$ (9.3%), and *iso*-$C_{15:0}$ (7.8%) (Table S1). The predominant respiratory quinone was identified as MK-7. These main chemotaxonomic properties were aligned with the typical characteristics of the genus *Saccharibacillus*.

Phylogenetic analysis

Based on the 16S rRNA gene sequence (1544 bp), JD154^T showed close similarities to *S. kuerlensis* DSM 22868^T (96.4%) and *S. sacchari* DSM 19268^T (96.4%) but still fell below the species differentiation threshold (98.65%) [35]. They formed a distinct clade in the phylogenetic tree, emphasizing its specific classification within the genus *Saccharibacillus* (Fig. 1).

Genome features

The sequenced genome of JD154^T was highly complete (with a completeness score of 98.62% and a contamination score of 1.23%), generated from 63 qualified scaffolds. It possessed a total of 5,290 coding genes, 54 tRNA genes, 5 other ncRNA genes, and 48 pseudogenes. The genome size was 6,275,545 bp with DNA G+C content being 59.2%. Both ANI values (< 80%) and dDDH values (< 23.4%) between strain JD154^T and other *Saccharibacillus* species were below the bacterial species differentiation threshold [28, 29] (Table S2). In the phylogenomic tree constructed

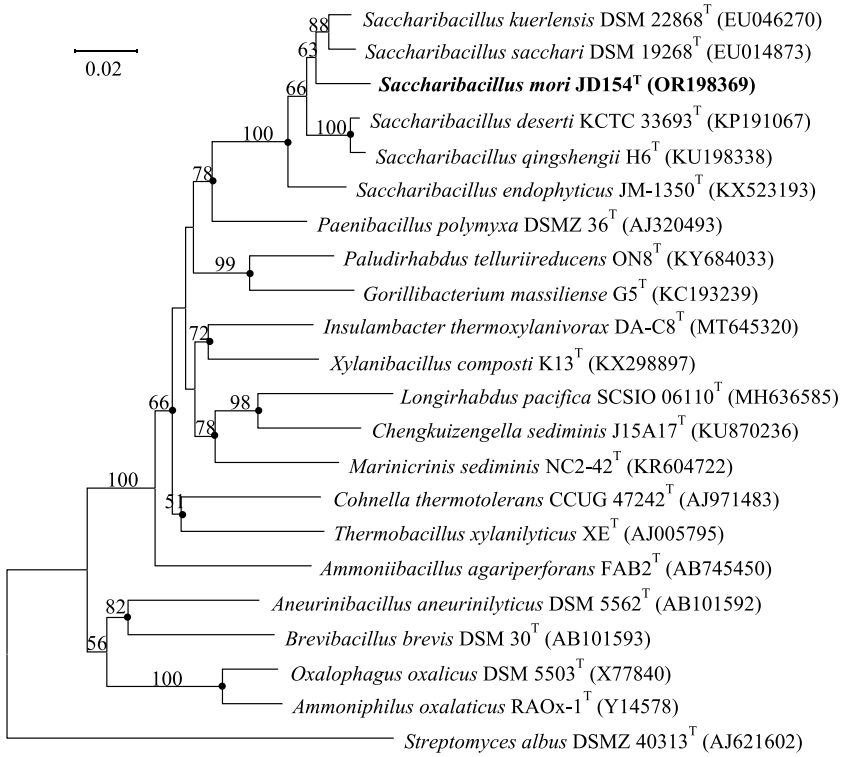

Fig. 1 Phylogenetic tree generated with neighbor-joining method based on the 16S rRNA gene sequences of strain JD154^T and the related strains of the family *Paenibacillaceae*. *Streptomyces albus* DSM 40313^T (AJ621602) was used as an outgroup. Bar, 0.02 substitutions per nucleotide position. Filled circles indicated that the corresponding nodes were also recovered in the trees generated with the maximum-likelihood and maximum parsimony methods.

based on core gene analysis, strain JD154^T was distinctly positioned within the cluster of the genus *Saccharibacillus* (Fig. S4).

The JD154^T genome encompassed genes involved in IAA biosynthetic pathways and phosphate uptake/-solubilization, showing its potential contribution to plant growth. The tryptophan-dependent pathways include the indole-3-acetamide (IAM), indole-3-pyruvic acid (IPyA), indole-3-acetonitrile (IAN), tryptamine (TAM), and tryptophan side-chain oxidase (TSO) pathways [36, 37], and the IAM, IPyA, and TAM pathways were found to be the main genes involved (Table S3). Additionally, the putative genes responsible for phosphate uptake and solubilization were also detected in the genome of strain JD154^T. Some of these genes such as alkaline phosphatase gene (*phoA*), phosphate-specific transporter gene (*pst*), alkaline phosphatase affinity transport system gene (*phn*), and glycerol-3-P uptaking gene (*ugp*) [38, 39] have been extensively investigated. Strain JD154^T harbored the phosphate transporter and conversion genes (*pstABCS*). These results indicated that strain JD154^T might have the potential to convert inorganic phosphate into a soluble form [38]. Furthermore, the presence of the *phnCDEP* gene cluster suggested that this strain could enhance phosphate uptake in plants, thus promoting plant growth. And the genome of strain JD154^T also contained the P-solubilization-related gene clusters *phoABHLU* and *ugpB* (Table S4) [39, 40]. A biosynthetic gene cluster (BGC) region that encoded a terpene compound was discovered between loci 174,060 bp and 194,953 bp (totaling 20,893 bp). The similarity between this BGC and that of carotenoids was 33%. Carotenoids play a crucial role in scavenging the superoxide anion radicals generated during the process of photosynthesis, owing to their ability to absorb and transfer electrons [41, 42]. The presence of the BGC hinted at the strain's ability to influence plant growth directly or indirectly.

Description of *Saccharibacillus mori* sp. nov.

Saccharibacillus mori can be described as mo′ri. L. gen. n. *mori* of a mulberry tree, of *Morus*, the generic name of the white mulberry, *Morus alba* L., from which the type strain, JD154^T (= CPCC 101409^T = KCTC 43346^T), was isolated (from a plant rhizosphere soil in Yunnan Province, China).

Cells are Gram-stain-positive with an approximate length of 2.0–3.9 μm and a width of 0.8–1.1 μm, and motile with lophotrichous flagella. Upon 48 h incubation at 28 °C, colonies on TSA medium are light-pink, convex, and opaque. Growth occurs on TSA within

Table 1 Differential physiological and biochemical comparison of strain JD154^T and the closely related type strains in the genus *Saccharibacillus*.

Characteristic	1	2	3
Temperature range for growth (°C)	10–37	15–42	4–42
pH	5–9	5–10	5–10
Salt tolerance (%)	0–7	0–5	0–8
Carbon source utilized for growth:			
3-Methyl Glucose	+	−	+
Acetoacetic Acid	−	+	+
Bromo-Succinic Acid	+	−	−
Citric Acid	+	−	−
D-Arabitol	+	−	−
D-Aspartic Acid	+	−	−
D-Cellobiose	−	+	−
Dextrin	−	+	+
D-Fructose	−	+	+
D-Fructose-6-PO4	+	−	−
D-Galactose	−	+	+
D-Galacturonic Acid	+	−	−
D-Gluconic Acid	−	+	+
D-Glucose-6-PO4	+	−	−
D-Glucuronic Acid	+	−	−
D-Lactic Acid Methyl Ester	+	−	−
D-Malic Acid	+	−	−
D-Maltose	−	+	+
D-Mannitol	−	+	−
D-Mannose	−	+	+
D-Melibiose	−	+	−
D-Raffinose	−	+	−
D-Saccharic Acid	+	−	−
D-Salicin	−	+	−
D-Serine	+	−	+
D-Sorbitol	+	−	+
D-Trehalose	−	+	−
Gelatin	+	−	−
Gentiobiose	−	+	−
Inosine	+	−	+
L-Alanine	+	−	−
L-Arginine	+	−	−
L-Aspartic Acid	+	−	−
L-Galactonic Acid Lactone	+	−	−
L-Glutamic Acid	+	−	−
L-Histidine	+	−	−
L-Malic Acid	+	−	−
L-Pyroglutamic Acid	+	−	−
Methyl Pyruvate	+	−	+
N-Acetyl Neuraminic Acid	+	−	−
N-Acetyl-D Galactosamine	+	−	−
N-Acetyl-D Glucosamine	−	−	+
Pectin	−	+	+
Stachyose	+	+	−
Sucrose	−	+	−
Tween 40	+	−	−
α-D-Glucose	−	+	−
α-D-Lactose	−	+	+
α-Keto-Butyric Acid	−	−	+
α-Keto-Glutaric Acid	+	−	−
β-Hydroxy-D, L-butyric Acid	+	−	−
β-Methyl-D Glucoside	−	+	−
γ-Amino-Butryric Acid	+	−	−
Enzyme activity of:			
Acid phosphatase	+	−	+
Esterase (C4)	−	+	+
Leucine arylamidase	−	w	+
α-Chymotrypsin	−	−	+
α-Galactosidase	+	−	+
β-Glucuronidase	+	−	+
API 50CH result:			
D-Arabinose	−	−	+
D-Ribose	−	+	+
D-Sorbitol	−	−	+
D-Turanose	+	−	+
Dulcitol	−	−	w
Glycerol	−	+	+
Inositol	−	+	+
Inulin	−	−	+
L-Fucose	−	−	+
L-Sorbose	−	−	+
L-Xylose	−	−	+
Methyl-α-D-Glucopyranoside	−	w	w
Methyl-β-D-Xylopyranoside	−	+	+
N-Acetylglucosamine	+	−	w
Xylitol	+	−	w

Strains: 1, JD154^T; 2, *S. kuerlensis* DSM 22868^T; and 3, *S. sacchari* DSM 19268^T. +, positive; −, negative; w, weakly positive. All data were from this study. All strains were positive to esterase lipase (C8), naphthol-AS-BI-phosphohydrolase, α-glucosidase, β-glucosidase, and β-galactosidase and negative to alkaline phosphatase, cystine arylamidase, lipase (C14), *N*-acetyl-β-glucosaminidase, trypsin, valine arylamidase, α-mannosidase, and β-fucosidase. All strains could produce acids from L-arabinose, amygdalin, arbutin, D-cellobiose, D-fructose, D-galactose, D-glucose, D-lactose, D-maltose, D-mannitol, D-mannose, D-melezitose, D-melibiose, D-raffinose, D-trehalose, D-xylose, esculin ferric citrate, gentiobiose, L-rhamnose, potassium gluconate, salicin, and sucrose. All strains could use D-turanose, fucose, glycerol, L-rhamnose, and *myo*-inositol as the sole carbon source.

a temperature range of 10–37 °C (optimum at 20–30 °C), a NaCl concentration between 0–7% (optimum at 0–1% NaCl), and at pH levels ranging from 5.0–9.0 (optimum at pH 7.0–8.0). Positive for catalase reaction, while negative for oxidase reaction, cellulose hydrolysis, starch hydrolysis, H_2S production, nitrate reduction, gelatin liquefaction, milk coagulation and peptonization, VP and MR tests. The polar lipids found in this strain are diphosphatidylglycerol and phosphatidylglycerol. The major respiratory quinone of the strain is MK-7. The fatty acid profile consists of *anteiso*-$C_{15:0}$, $C_{16:0}$, *iso*-$C_{14:0}$, and *iso*-$C_{15:0}$ as the predominant components (> 5%). The type strain, JD154^T (= CPCC 101409^T = KCTC 43346^T), was isolated from a medicinal plant rhizosphere soil in Yunnan Province, China. The genome size of strain JD154^T is 6.3 Mbp and the genomic G+C content is 59.2%.

CONCLUSION

The comprehensive phenotypic and genotypic criteria effectively differentiated strain JD154^T from other

validly described *Saccharibacillus* species. Compelling results support the designation of isolate JD154^{T} as a new species of *Saccharibacillus*, dubbed *Saccharibacillus mori* sp. nov. Moreover, the presence of genes involved in hormone biosynthesis and phosphate solubilization pathways indicated that the strain could function as a plant growth promoting (PGP) bacterium. This discovery could have significant implications not just for taxonomical purposes but potentially in agricultural applications as well, considering the PGP potentials of strain JD154^{T}. Continuation of research in this area could unveil more about its capacities to promote plant growth and thereby contribute to sustainable agricultural practices.

Appendix A. Supplementary data

Supplementary data associated with this article can be found at http://dx.doi.org/10.2306/scienceasia1513-1874.2024.047.

Acknowledgements: This research was supported by National Natural Science Foundation of China (32170021), CAMS Innovation Fund for Medical Sciences (CIFMS, 2021-I2M-1-055), Beijing Natural Science Foundation (5212018), Key project at central government level-the ability establishment of sustainable use for valuable Chinese medicine resources (2060302) and the National Infrastructure of Microbial Resources (NIMR-2021-3).

REFERENCES

1. Rivas R, García-Fraile P, Zurdo-Piñeiro JL, Mateos PF, Martínez-Molina E, Bedmar EJ, Sánchez-Raya J, Velázquez E (2008) *Saccharibacillus sacchari* gen. nov., sp. nov., isolated from sugar cane. *Int J Syst Evol Microbiol* **58**, 1850–1854.
2. Sun JQ, Wang XY, Wang LJ, Xu L, Liu M, Wu XL (2016) *Saccharibacillus deserti* sp. nov., isolated from desert soil. *Int J Syst Evol Microbiol* **66**, 623–627.
3. Yang SY, Liu H, Liu R, Zhang KY, Lai R (2009). *Saccharibacillus kuerlensis* sp. nov., isolated from a desert soil. *Int J Syst Evol Microbiol* **59**, 953–957.
4. Han H, Gao S, Wang Q, He LY, Sheng XF (2016) *Saccharibacillus qingshengii* sp. nov., isolated from a lead-cadmium tailing. *Int J Syst Evol Microbiol* **66**, 4645–4649.
5. Kämpfer P, Busse HJ, Kleinhagauer T, McInroy JA, Glaeser SP (2016) *Saccharibacillus endophyticus* sp. nov., an endophyte of cotton. *Int J Syst Evol Microbiol* **66**, 5134–5139.
6. Bziuk N, Maccario L, Straube B, Wehner G, Sørensen SJ, Schikora A, Smalla K (2021) The treasure inside barley seeds: microbial diversity and plant beneficial bacteria. *Environ Microbiome* **16**, 20.
7. Jiang ZM, Zhang BH, Sun HM, Zhang T, Yu LY, Zhang YQ (2021) Properties of *Modestobacter deserti* sp. nov., a kind of novel phosphate-solubilizing actinobacteria inhabited in the desert biological soil crusts. *Front Microbiol* **12**, 742798.
8. Li WJ, Xu P, Schumann P, Zhang YQ, Pukall R, Xu LH, Stackebrandt E, Jiang CL (2007) *Georgenia ruanii* sp. nov., a novel actinobacterium isolated from forest soil in Yunnan (China), and emended description of the genus *Georgenia*. *Int J Syst Evol Microbiol* **57**, 1424–1428.
9. Tamura K, Stecher G, Kumar S (2021) MEGA11: Molecular evolutionary genetics analysis version 11. *Mol Biol Evol* **38**, 3022–3027.
10. Saitou N, Nei M (1987) The neighbor-joining method: a new method for reconstructing phylogenetic trees. *Mol Biol Evol* **4**, 406–425.
11. Kimura M (1980) A simple method for estimating evolutionary rates of base substitutions through comparative studies of nucleotide sequences. *J Mol Evol* **16**, 111–120.
12. Kimura M (1979) The neutral theory of molecular evolution. *Sci Am* **241**, 98–126.
13. Kluge AG, Farris JSJSB (1969) Quantitative phyletics and the evolution of anurans. *Syst Zool* **18**, 1–32.
14. Felsenstein J (1981) Evolutionary trees from DNA sequences: a maximum likelihood approach. *J Mol Evol* **17**, 368–376.
15. Felsenstein J (1985) Confidence limits on phylogenies: an approach using the bootstrap. *Evolution* **39**, 783–791.
16. Shirling ET, Gottlieb D (1966) Methods for characterization of *Streptomyces* species. *Int J Syst Bacteriol* **16**, 313–340.
17. Bernardet JF, Nakagawa Y, Holmes B (2002) Proposed minimal standards for describing new taxa of the family *Flavobacteriaceae* and emended description of the family. *Int J Syst Evol Microbiol* **52**, 1049–1070.
18. Dong L, Ming H, Yin YR, Duan YY, Zhou EM, Nie GX, Feng HG, Liu L, et al (2014) *Roseomonas alkaliterrae* sp. nov., isolated from an alkali geothermal soil sample in Tengchong, Yunnan, South-West China. *Antonie Van Leeuwenhoek* **105**, 899–905.
19. Barry AL, Feeney KL (1967) Two quick methods for Voges-Proskauer test. *Appl Microbiol* **15**, 1138–1141.
20. Barry AL, Bernsohn KL, Adams AP, Thrupp LD (1970) Improved 18-hour methyl red test. *Appl Microbiol* **20**, 866–870.
21. Bric JM, Bostock RM, Silverstone SE (1991) Rapid *in situ* assay for indoleacetic acid production by bacteria immobilized on a nitrocellulose membrane. *Appl Environ Microbiol* **57**, 535–538.
22. Jiang ZM, Deng Y, Han XF, Su J, Wang H, Yu LY, Zhang YQ (2022) *Geminicoccus flavidas* sp. nov. and *Geminicoccus harenae* sp. nov., two IAA-producing novel rare bacterial species inhabiting desert biological soil crusts. *Front Microbiol* **13**, 1034816.
23. Qiao CC, Wang TT, Wang RF, Liu C, Gao Q, Li R, Shen QR (2017) Screening phosphate solubilizing bacterial strains from maize rhizosphere and research on their plant growth promotion effect. *J Nanjing Agric Univ* **40**, 664–670.
24. Minnikin DE, Odonnell AG, Goodfellow M, Alderson G, Athalye M, Schaal A, Parlett JH (1984) An integrated procedure for the extraction of bacterial isoprenoid quinones and polar lipids. *J Microbiol Methods* **2**, 233–241.
25. Collins MD, Pirouz T, Goodfellow M, Minnikin DE (1977) Distribution of menaquinones in actinomycetes and corynebacteria. *J Gen Microbiol* **100**, 221–230.
26. Groth I, Schumann P, Rainey FA, Martin K, Schuetze B, Augsten K (1997) *Demetria terragena* gen. nov., sp. nov., a new genus of actinomycetes isolated from compost soil. *Int J Syst Bacteriol* **47**, 1129–1133.

27. Kroppenstedt RM (1985) Fatty acid and menaquinone analysis of actinomycetes and related organisms. In: Goodfellow M, Minnikin DE (eds) *Chemical Methods in Bacterial Systematics*, vol 20, Society for applied bacteriology technical series. Academic Press, Manhattan NY, pp 173–199.
28. Auch AF, von Jan M, Klenk HP, Göker M (2010) Digital DNA-DNA hybridization for microbial species delineation by means of genome-to-genome sequence comparison. *Stand Genomic Sci* **2**, 117–134.
29. Yoon SH, Ha SM, Lim J, Kwon S, Chun J (2017) A large-scale evaluation of algorithms to calculate average nucleotide identity. *Antonie Van Leeuwenhoek* **110**, 1281–1286.
30. Zhang DF, Cui XW, Zhao Z, Zhang AH, Huang JK, Li WJ (2020) *Sphingomonas hominis* sp. nov., isolated from hair of a 21-year-old girl. *Antonie Van Leeuwenhoek* **113**, 1523–1530.
31. Nguyen LT, Schmidt HA, von Haeseler A, Minh BQ (2015) IQ-TREE: a fast and effective stochastic algorithm for estimating maximum-likelihood phylogenies. *Mol Biol Evol* **32**, 268–274.
32. Chan PP, Lin BY, Mak AJ, Lowe TM (2021) tRNAscan-SE 2.0: improved detection and functional classification of transfer RNA genes. *Nucleic Acids Res* **49**, 9077–9096.
33. Kanehisa M, Sato Y, Kawashima M, Furumichi M, Tanabe M (2016) KEGG as a reference resource for gene and protein annotation. *Nucleic Acids Res* **44**, D457–D462.
34. Blin K, Shaw S, Augustijn HE, Reitz ZL, Biermann F, Alanjary M, Fetter A, Terlouw BR, et al (2023) antiSMASH 7.0: new and improved predictions for detection, regulation, chemical structures and visualisation. *Nucleic Acids Res* **51**, W46–W50.
35. Kim M, Oh HS, Park SC, Chun J (2014) Towards a taxonomic coherence between average nucleotide identity and 16S rRNA gene sequence similarity for species demarcation of prokaryotes. *Int J Syst Evol Microbiol* **64**, 346–351.
36. Duca D, Lorv J, Patten CL, Rose D, Glick BR (2014) Indole-3-acetic acid in plant-microbe interactions. *Antonie van Leeuwenhoek* **106**, 85–125.
37. Di DW, Zhang C, Luo P, An CW, Guo GQ (2016) The biosynthesis of auxin: how many paths truly lead to IAA? *Plant Growth Regul* **78**, 275–285.
38. Song Y, Jiang CY, Liang ZL, Wang BJ, Jiang Y, Yin Y, Zhu HZ, Qin YL, et al (2020) *Casimicrobium huifangae* gen. nov., sp. nov., a ubiquitous "most-wanted" core bacterial taxon from municipal wastewater treatment plants. *Appl Environ Microbiol* **86**, e02209-19.
39. Li H, Li M, Huang Y, Rensing C, Wang G (2013) *In silico* analysis of bacterial arsenic islands reveals remarkable synteny and functional relatedness between arsenate and phosphate. *Front Microbiol* **4**, 347.
40. Petriglieri F, Singleton C, Peces M, Petersen JF, Nierychlo M, Nielsen PH (2021) "*Candidatus Dechloromonas phosphoritropha*" and "Ca. D. *phosphorivorans*", novel polyphosphate accumulating organisms abundant in wastewater treatment systems. *ISME J* **15**, 3605–3614.
41. Bartley GE, Scolnik PA (1995) Plant carotenoids: pigments for photoprotection, visual attraction, and human health. *Plant Cell* **7**, 1027–1038.
42. Satchasataporn K, Duangsri C, Charunchaipipat W, Laloknam S, Burut-Archanai S, Powtongsook S, Raksajit W (2022) Enhanced production of poly-3-hydroxybutyrate and carotenoids by Arthrospira platensis under combined glycerol and phosphorus supplementation. *ScienceAsia* **48**, 509–517.

Appendix A. Supplementary data

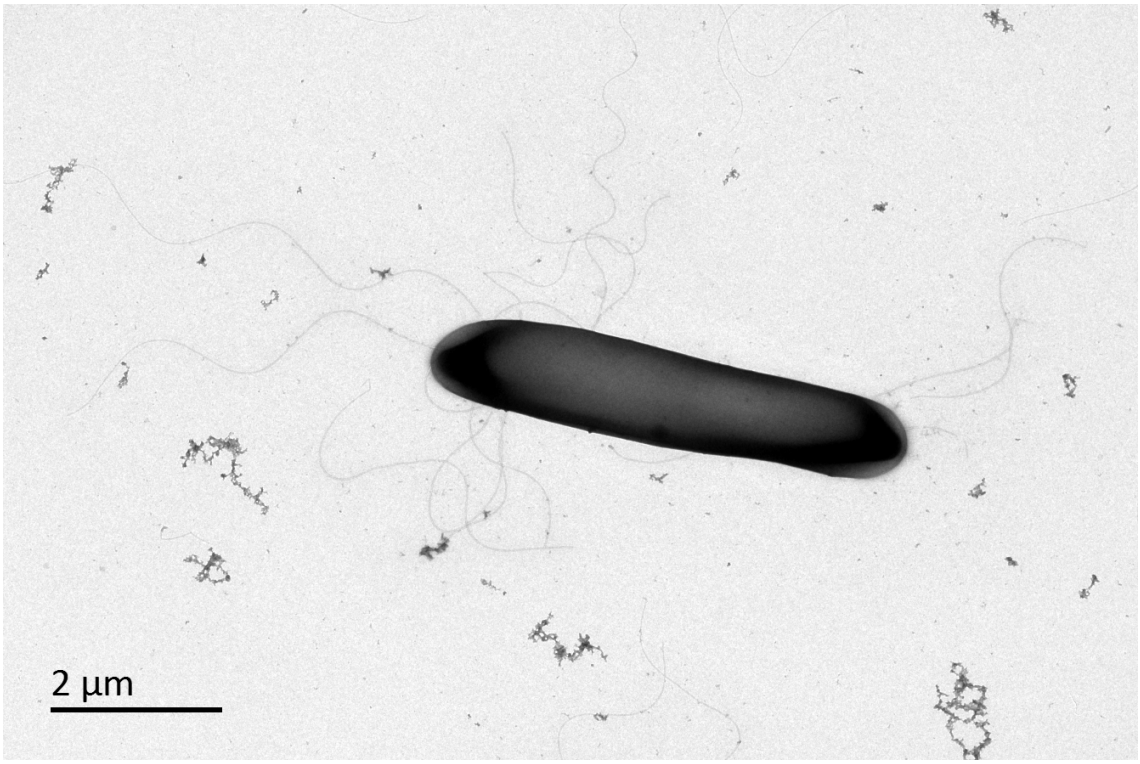

Fig. S1 Transmission electron micrograph of the motile cell of strain JD154^{T}.

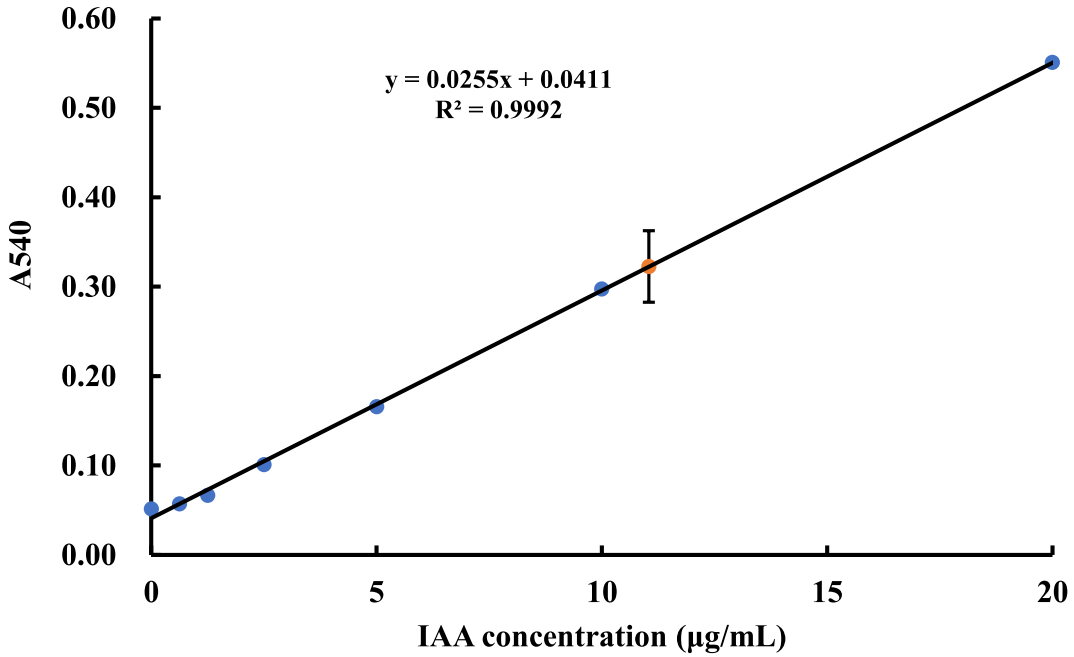

Fig. S2 IAA standard curve and the absorbance value of strain JD154^{T}. The circle colored in orange represented the absorbance value of the strain JD154^{T}.

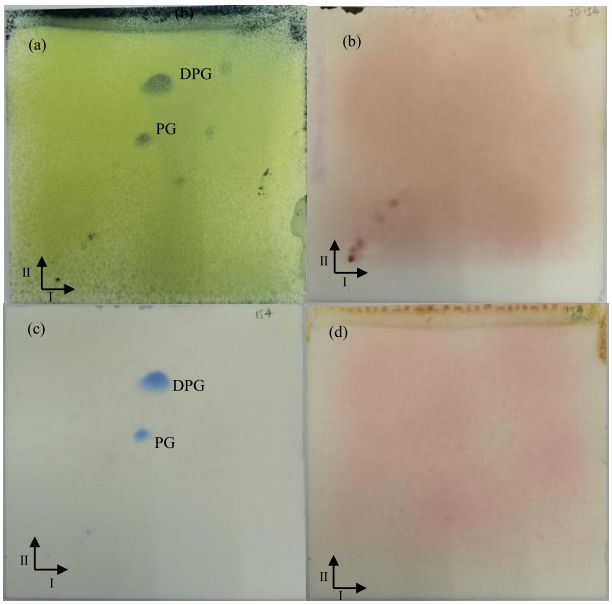

Fig. S3 Polar lipid profiles for strain JD154^{T} after separation by two-dimensional TLC. Detection by spraying with (a) molybdatophosphoric acid reagent, (b) ninhydrin stain reagent, (c) molybdenum blue stain reagent, and (d) p-anisaldehyde stain reagent. DPG, diphosphatidylglycerol; PG, phosphatidylglycerol.

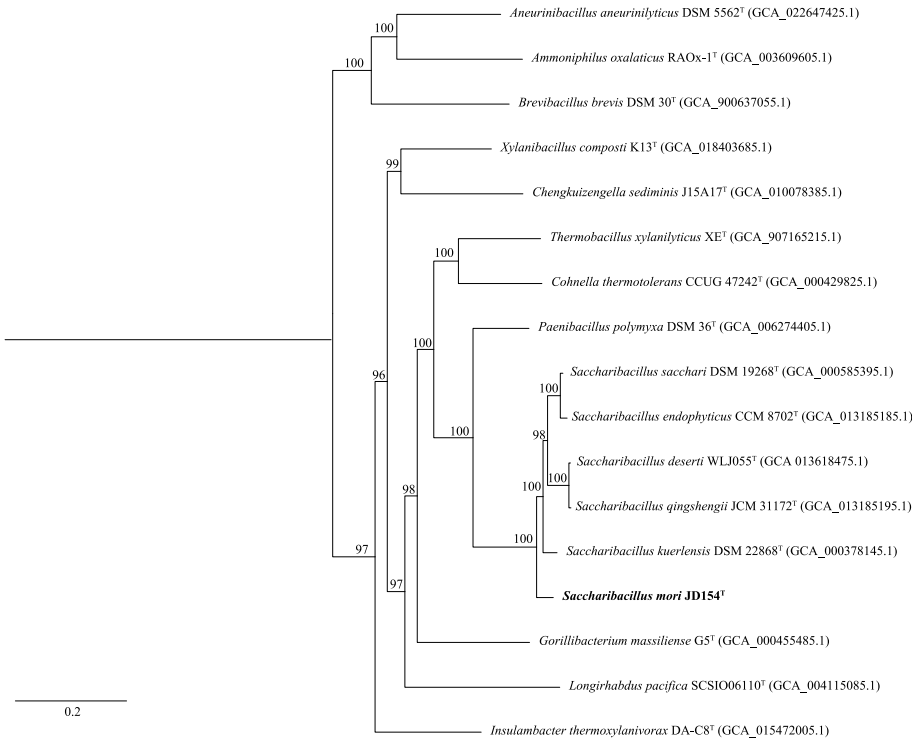

Fig. S4 Maximum-likelihood core gene phylogenetic tree based on protein sequences of the genomes of strain JD154^{T} and related strains of the family *Paenibacillaceae*. Bootstrap values are shown at the branch points nodes. RefSeq assembly accession number is indicated in the bracket. *Insulambacter thermoxylanivorax* DA-C8T (RefSeq assembly accession no. GCA_015472005.1) is used as an outgroup (not shown in Figure). Bar, 0.2 substitutions per protein position.

Table S1 Cellular fatty acid content (> 1.0%) of strain JD154^T and the reference type strains of the genus *Saccharibacillus*.

Fatty acid	1	2	3
Saturated fatty acid			
C14:0	2.7	3.9	7.6
C16:0	12.0	21.7	25.2
iso-$C_{14:0}$	9.3	6.6	7.7
iso-$C_{15:0}$	7.8	2.2	3.0
iso-$C_{16:0}$	7.0	3.6	6.3
iso-$C_{17:0}$	1.3	1.1	0.8
anteiso-$C_{15:0}$	52.8	50.4	45.2
anteiso-$C_{17:0}$	2.0	4.8	2.3
Unsaturated fatty acid			
$C_{16:1}$ ω11c	–	5.6	–

Strains: 1, JD154^T; 2, *S. kuerlensis* DSM 22868^T; and 3, *S. sacchari* DSM 19268^T. –, not detected.

Table S2 The ANI and dDDH values between strain JD154^T and other related type strains of the genus *Saccharibacillus*.

	1	2	3	4	5	6
1	–	**17.7**	**20.0**	**23.4**	**21.0**	**23.1**
2	77.1	–	**19.4**	**23.0**	**19.6**	**22.3**
3	77.9	77.4	–	**24.1**	**78.7**	**24.6**
4	80.0	78.1	78.5	–	**25.5**	**76.2**
5	78.0	77.4	91.4	78.9	–	**25.7**
6	78.9	78.3	78.7	94.4	78.8	–

Strains: 1, JD154^T; 2, *S. kuerlensis* DSM 22868^T; 3, *S. sacchari* DSM 19268^T; 4, *S. deserti* KCTC 33693^T; 5, *S. endophyticus* JM-1350^T; and 6, *S. qingshengii* H6^T. Values in bold forms were the dDDH, and ones in normal forms were ANI.

Table S3 Genomic analysis of indole-3-acetic acid (IAA) biosynthesis pathways in strain JD154^T.

Pathway	Enzyme	JD154^T
Indole-3-acetamide (IAM)	Trypthophan 2-monooxygenase (EC:1.13.12.3)	–
	Amidase (EC:3.5.1.4)	+
Indole-3-pyruvic acid (IPyA)	Trp aminotransferase (EC:2.6.1.27)	–
	Indolepyruvate decarboxylase (EC:4.1.1.74)	+
	Aldehyde dehydrogenase (EC:1.2.1.3)	+
Tryptamine (TAM)	Trp decarboxylase (EC:4.1.1.28)	–
	Monoamine oxidase (EC:1.4.3.4)	–
	Aldehyde dehydrogenase (EC:1.2.1.3)	+

Table S4 Genes involved in phosphate solubilization in the genome of strain JD154^T.

Gene	Gene annotation	E.C. Number
phnD	Phosphonate transport system substrate-binding protein	
phnC	Phosphonate transport system ATP-binding protein	[EC:7.3.2.2]
phnE	Phosphonate transport system permease protein	
phnP	Phosphoribosyl 1,2-cyclic phosphate phosphodiesterase	[EC:3.1.4.55]
phoA, *phoB*	Alkaline phosphatase	[EC:3.1.3.1]
phoH, *phoL*	Phosphate starvation-inducible protein PhoH and related proteins	
phoU	Phosphate transport system protein	
pstA	Phosphate transport system permease protein	
pstB	Phosphate transport system ATP-binding protein	[EC:7.3.2.1]
pstC	Phosphate transport system permease protein	
pstS	Phosphate transport system substrate-binding protein	
ptsH	Phosphocarrier protein HPr	
ugpB	Sn-glycerol 3-phosphate transport system substrate-binding protein	